

An Homomorphic Filtering And Expectation Maximization Approach For The Point Spread Function Estimation In Ultrasound Imaging

S. Benameur^a, M. Mignotte^b and F. Lavoie^a

^aEiffel Medtech Inc., Montréal, Québec, Canada;

^bDépartement d'Informatique et de Recherche Opérationnelle, Université de Montréal, Québec, Canada

ABSTRACT

In modern ultrasound imaging systems, the spatial resolution is severely limited due to the effects of both the finite aperture and overall bandwidth of ultrasound transducers and the non-negligible width of the transmitted ultrasound beams. This low spatial resolution remains the major limiting factor in the clinical usefulness of medical ultrasound images. In order to recover clinically important image details, which are often masked due to this resolution limitation, an image restoration procedure should be applied. To this end, an estimation of the Point Spread Function (PSF) of the ultrasound imaging system is required. This paper introduces a novel, original, reliable, and fast Maximum Likelihood (ML) approach for recovering the PSF of an ultrasound imaging system. This new PSF estimation method assumes as a constraint that the PSF is of known parametric form. Under this constraint, the parameter values of its associated Modulation Transfer Function (MTF) are then efficiently estimated using a homomorphic filter, a denoising step, and an expectation-maximization (EM) based clustering algorithm. Given this PSF estimate, a deconvolution can then be efficiently used in order to improve the spatial resolution of an ultrasound image and to obtain an estimate (independent of the properties of the imaging system) of the true tissue reflectivity function. The experiments reported in this paper demonstrate the efficiency and illustrate all the potential of this new estimation and blind deconvolution approach.

Keywords: Restoration / deconvolution, Expectation-Maximization (EM), Point Spread Function (PSF) estimation, ultrasound images.

1. INTRODUCTION

Contrary to other medical imaging techniques (e.g., X-rays, magnetic resonance imaging, and computerized tomography), ultrasound imagery is currently considered to be a non-invasive, portable, non-expensive and safe (for the patient and operator) visualization medical tool for investigating biological tissues of a body. However, despite considerable advances in the technology of ultrasound imaging equipment over the last years, the primary limitation of this imaging modality remains its poor image quality (i.e., low signal-to-noise ratio, low resolution and contrast), and also the presence of artifacts due to the speckle noise effect that drastically deteriorates image quality and sometimes makes imperceptible clinically important details within these images (such as contours of anatomical structures).

In order to improve the quality of such ultrasound images, an image deconvolution/restoration procedure could be efficiently applied and, to this end, given a PSF estimate, many deconvolution models exist.¹ The only requirement for such deconvolution algorithms consists, as a prerequisite first stage, of an estimation of the PSF of the underlying ultrasound imaging system. This problem of estimating the PSF and restoring is called a *blind deconvolution* process and an alternative approach to this above-mentioned estimation and deconvolution (disjoint) procedures consists of the simultaneous (generally iterative) estimation of the undegraded original image and the PSF (or its inverse).²⁻⁵

Further author information: (Send correspondence to S. Benameur)

S. Benameur: E-mail: benameus@iro.umontreal.ca, Telephone: 1 514 380 8666

F. Lavoie: E-mail: flavoie@eiffelmedtech.com, Telephone: 1 514 380 8666

Image Processing: Algorithms and Systems X; and Parallel Processing for Imaging Applications II, edited by Karen O. Egiazarian, Sos S. Agaian, Atanas P. Gotchev, John Recker, Guijin Wang, Proc. of SPIE-IS&T Electronic Imaging, SPIE Vol. 8295, 82950T • © 2012 SPIE-IS&T • CCC code: 0277-786X/12/\$18 • doi: 10.1117/12.903785

Amongst the first blind deconvolution strategy for which estimating the PSF estimation and the restoration process are two disjoint procedures, we can cite the PSF identification procedure based on frequency domain zeros⁶ or the homomorphic filtering method which consists in low-pass filtering (also called *liftering*) in the complex cepstral domain (the cepstrum being defined by the inverse Fourier transform of the log of the spectrum). This low-pass filtering is commonly achieved either with an ideal low-pass filter^{7,8} or by hard or a soft shrinkage rule in the wavelet domain.⁹ It is also worth mentioning the estimation approach by means of local polynomial approximation proposed by Adam and Michailovich,¹⁰ which can be viewed as a modification of homomorphic estimation by using wavelet bases instead of the Fourier basis. Nevertheless, ideal low-pass filtering in the cepstral domain or by other wavelet-based *liftering* procedures have several drawbacks. First, they are highly supervised to adequately set the cutoff frequency parameter which is crucial and different for each ultrasound image because of the spatial variability of the PSF (due to the presence of different interrogated tissues between the transducer and the anatomical structure to be imaged). Second, these classical *liftering* methods are not robust enough to give a good estimate of the PSF spectrum and often tend to produce artifacts in this estimation mainly due to the ringing effect of such ideal low pass filter in the Fourier domain or due to the *blocky* effect inherent to the wavelet based *liftering* procedure.

In this paper, we propose an original, simple, and fast PSF estimation strategy that remedies these above-mentioned problems and which is based on an additional constraint, namely that the PSF to be estimated is of known parametric form. With a homomorphic filtering approach and a denoising step, this constraint amounts to estimating, in the low-pass-filtered cepstral domain, a mixture of two identical Gaussian distributions whose parameters are automatically estimated, in a Maximum Likelihood sense, by an iterative expectation-maximization (EM¹¹) based clustering algorithm. Given this PSF estimate, we show that a deconvolution algorithm can then be efficiently used, in a subsequent stage, in order to improve the spatial resolution of the ultrasound images and to obtain an estimate of the true tissue reflectivity function which is then independent of the properties of the ultrasound system.

2. PSF ESTIMATION BY HOMOMORPHIC TRANSFORMATION

2.1 General Concept

Assuming space invariance* and linearity, the resolution capabilities of an ultrasound imaging system can be expressed in terms of the PSF, $h(x, y)$, i.e., the image of a point reflector, by the following classical linear model:

$$g(x, y) = f(x, y) * h(x, y) + n(x, y) \quad (1)$$

where $f(x, y)$ is the spatial reflectance distribution of internal organs of the human body to be imaged, $g(x, y)$ is the degraded ultrasound image of the object $f(x, y)$, $h(x, y)$ is the PSF function of the imaging system, which counts for the finite aperture and bandwidth of the transducer, $n(x, y)$ describes the additive quantization and electronic noise and finally $*$ designates the 2D discrete linear convolution operator. Assuming that the noise term $n(x, y)$ is temporarily ignored for the sake of simplicity, Eq. (1) is more easily described in frequency domain as a simple product and sum where the capital letters indicate the Fourier transforms of the corresponding spatial functions:

$$G(u, \nu) = F(u, \nu) H(u, \nu) \quad (2)$$

An homomorphic transformation is simply the complex logarithmic transformation of both side of Eq. (2). The real (**Re**) and the imaginary (**Im**) parts of the resultant relation are given correspondingly by:

$$\mathbf{Re} : \quad \log |G(u, \nu)| \simeq \log |F(u, \nu)| + \log |H(u, \nu)| \quad (3)$$

$$\mathbf{Im} : \quad \angle G(u, \nu) \simeq \angle F(u, \nu) + \angle H(u, \nu) \quad (4)$$

*In ultrasound imaging, the PSF happens to exhibit spatial dependency due, among other things, to the non-uniformity of focusing, the dispersive attenuation and the heterogeneity of the different interrogated tissues. Nevertheless, a relatively low spatial variability of these phenomena makes it possible to divide the obtained acoustic image into a predefined number of small enough (possible overlapping) images, for which we can consider the data within each one to be quasi-stationary, with a different PSF.⁸ It is then assumed that, the entire image can be easily recovered by combining all the local results obtained in this manner.⁹

where the symbol $|\cdot|$ and \angle denote the amplitude and the phase of the complex functions respectively. The basis idea for cepstrum-based methods of estimating the PSF spectrum $H(u, \nu)$ relies in the fact that $\log |H(u, \nu)|$ is typically a much smoother function than $\log |F(u, \nu)|$ and the same holds for the functions $\angle H(u, \nu)$ and $\angle F(u, \nu)$. Consequently, in this context, the log-spectrum of the degraded ultrasound image (amplitude and phase) is considered to be a noisy version of the complex log-spectrum of the PSF to be estimated⁷⁻⁹ and in this setting, in which $\log |F(u, \nu)|$ and $\angle F(u, \nu)$ are considered to be sources of noise to be rejected, the problem of recovering $\log |H(u, \nu)|$ and $\angle H(u, \nu)$ is thus essentially a denoising problem in the cepstral domain.

2.2 Denoising Step

In order to ensure both an automatic procedure and also a reliable denoising step allowing a good estimate of the PSF spectrum, $H(u, \nu)$, without (ringing or blocking) artifacts, we herein propose a two-stage denoising scheme; namely a DCT-based denoising step using a hard thresholding rule followed by a EM-based regression model. In addition, since our PSF model relies on an even function in x and y , the phase spectrum is assumed to be null.

2.3 DCT-based Denoising Step

Algorithmically, our iterative DCT-based denoising procedure (see Algorithm I and¹²) thus simply consists in applying iteratively, until a maximal number of iterations is reached or until convergence is achieved, a frequential filtering based on the DCT transform of each 8×8 sub-image extracted from the current version of the image to be denoised (initially, this current image estimate is the noisy image itself). For the filtering operation in the DCT domain, we have chosen the easily-implemented hard thresholding rule¹³ also classically used in wavelet based denoising approaches, where ϵ is a threshold level and w is one of the coefficients obtained by the DCT transform of the block (of size 8×8 pixels) extracted from the current image to be denoised. In order to reduce blocky artifacts across block boundaries, we adopted a standard approach where this transform is made translation-invariant, by using the DCT of all (circularly) translated version of each channel of the image (herein assumed to be toroidal)¹⁴ (this implies computing a set of 8 horizontal shifts and 8 vertical shifts transformed images) which will then be averaged at each step of this iterative denoising procedure. In order to speed up the procedure, we use an overlap of three pixels for the sliding 8×8 window. This iterative denoising procedure is applied on the noisy version of $\log H(u, \nu)$, i.e., $\log G(u, \nu)$ (amplitude and phase) and allows us to obtain a first rough estimate of $\log \hat{H}(u, \nu)$ which will be refined in the next step.

2.4 EM-based Estimation Step

In order to refine the estimation given by the above-mentioned denoising step, our estimation method now relies on an additional constraint, namely that the PSF to be estimated has the following parametric form:

$$h(x, y) = \exp\left[-\left(\frac{x^2}{2\sigma_x^2} + \frac{y^2}{2\sigma_y^2}\right)\right] \cos(2\pi f_0 y) \quad (5)$$

which is the PSF model used in,¹⁵ i.e. a symmetric (across the x-axis and y-axis) cosine modulated by a Gaussian envelope whose the Fourier spectrum, i.e., its MTF (in fact a band-pass filter), namely $H(u, \nu)$ can be written in the Fourier domain:

$$H(u, \nu) = \pi\sigma_x\sigma_y \exp(-2\pi^2\sigma_x^2 u^2) \left\{ \exp\{-2\pi^2\sigma_y^2 (\nu - f_0)^2\} + \exp\{-2\pi^2\sigma_y^2 (\nu + f_0)^2\} \right\}$$

Under this constraint, we can now consider the regression model that gives, for the set of amplitude values of $|\hat{H}(u, \nu)|$, the best fit, in the least square sense, of two equally weighted Gaussian distributions (with the constraints that these two distributions are centered at $u = 0$ and symmetric with respect to ν). In that prospect, this latter regression model can be efficiently addressed by considering the parameter statistical estimation problem of a (noisy) Gaussian distribution mixture of two (equally weighted) Gaussian component in R^2 by considering N_f 2-dimensional vectors $\mathbf{v} = (u, \nu)^t$, $\mathbf{v} = \{\mathbf{v}_i, 1 \leq i \leq N_f\}$, taking their values in R^2 and whose cardinality of each \mathbf{v} is given by the amplitude value $\hat{H}(u, \nu)$. Finally, we assume that $\mathbf{v} = \mathbf{v}_1, \dots, \mathbf{v}_{N_f}$ is a realization in, R^2 , of \mathbf{V} whose density takes the form of the following 2-component mixture:

$$P_{\mathbf{V}}(\mathbf{v}) = \sum_{k=1}^2 p_k P_{\mathbf{V}/C}(\mathbf{v}/c_k, \Psi_k). \quad (6)$$

Algorithm 1 : DCT-Based Denoising Step

$I^{[n]}$ Input image to be denoised at iteration n
 $\hat{I}^{[n]}$ Denoised estimated image at iteration n
 ϵ Threshold

for All (8 horiz. and 8 vert.) shifts of $I^{[n]}$ **do**

for All 8×8 blocks extracted from $I^{[n]}$ **do**

1. DCT Transform

2. Threshold the obtained DCT coefficients w with the hard thresholding rule

$$w_{\text{hard}_\epsilon} = \begin{cases} 0 & \text{if } |w| \leq \epsilon \\ w & \text{otherwise} \end{cases}$$

3. Inverse DCT of these thresholded coefficients

▷ Unshift the filtered image and store it

$\hat{I}^{[n]} \leftarrow$ Averaging of these 64 denoised images

in which, the 2 components $P_{\mathbf{V}/C_i}(\mathbf{v}/c_k, \Psi_k)$ are, in our application (see Eq. (5)) assumed to be two equally weighted ($p_1 = p_2 = 0.5$) bi-variate Gaussian distributions with mean vector μ_k and identical covariance matrix Σ ($\Psi_k = (\mu_k, \Sigma)$), i.e.:

$$P_{\mathbf{V}/C_i}(\cdot) = \frac{1}{2\pi} |\Sigma|^{\frac{1}{2}} \exp\left\{-\frac{1}{2}(\mathbf{v} - \mu_k)^t \Sigma^{-1}(\mathbf{v} - \mu_k)\right\}.$$

In this setting, the identification of the parameters of the PSF spectrum modulus $H(u, \nu)$ amounts to estimate the parameters (Ψ_1 and Ψ_2 with the constraints that these two distributions are centered at $u = 0$ ($\mu_1 = (u = 0, \nu_1)^t$ and $\mu_2 = (u = 0, \nu_2)$) and ν_1 and ν_2 symmetric with respect to $\nu = 0$, i.e., of opposite sign. This 2-component Gaussian mixture model is estimated thanks to a EM-based clustering algorithm,¹¹ whose the initial parameters of this iterative procedure are given by the ML estimation on the partition given by a simple K-means clustering procedure. The constrain of identical covariance matrix and mean vector centered at $u = 0$ are taken into account at the end of this procedure by simply considering the average value of the two covariance matrices and the average absolute value of ν_1 and ν_2 .

3. DECONVOLUTION

In order to improve the spatial resolution of the ultrasound images and to obtain an estimate of the true tissue reflectivity function, we can now deconvolve out the ultrasound system's point-spread function. In our application, we have used an unsupervised Bayesian deconvolution approach¹⁶ (or a penalized likelihood framework) exploiting a non-parametric adaptive prior distribution derived from the recent image model proposed by Buades in.¹⁷ This prior expresses that acceptable deconvolved solutions are the images exhibiting a high degree of redundancy. In this setting, the deconvolution of ultrasound images leads to the following cost function to be optimized:

$$E(f) = \|g - h * f\| + \rho \|f - \Upsilon_{[g]}(f)\| \quad (7)$$

where the first term expresses the fidelity to the available data g and the second encodes the expected property of the true undegraded image and $\Upsilon_{[g]}(f)$ designates the non-local means filter¹⁷ applied on f . ρ , the regularization

parameter controlling the contribution of the two terms (which is crucial in the determination of the overall quality of the final estimate), is estimated with the method proposed in.¹⁶

4. EXPERIMENTAL RESULTS

In all experiments, we have tested our PSF estimation approach and deconvolution on ultrasound images of several bones acquired using a portable B-mode ultrasound imaging system (Titan, SonoSite, Bothell, WA, USA). The echographic appearance of the various tissues ranges from dark (low-echoic) to bright (high-echoic), depending on their acoustic impedance (see Fig. 1).

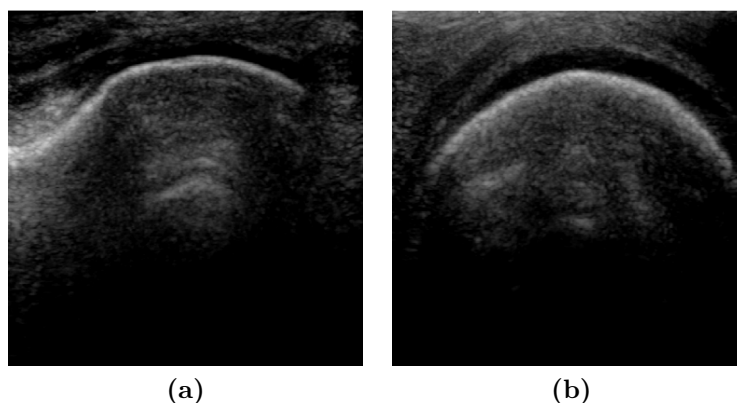


Figure 1. Original ultrasound images of the distal femur. (a) Medial side, coronal plane. (b) Medial posterior condyle, axial plane.

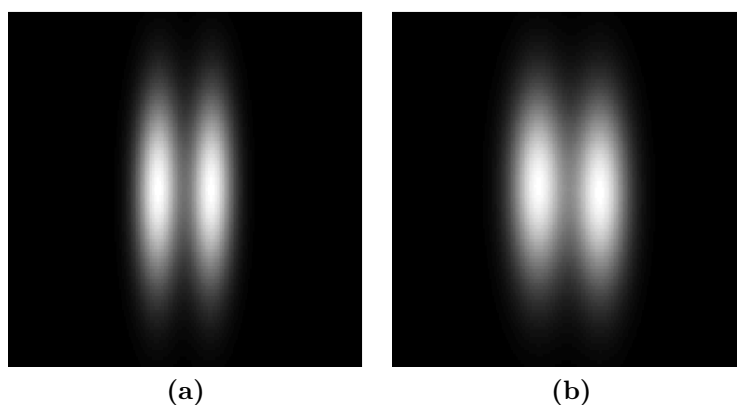


Figure 2. Modulus of $\hat{H}(u, \nu)$ after the DCT-based denoising step (see Section 2.3) for respectively : (a) Fig.1a, (b) Fig.1b.

Figure 2 shows the modulus of $\hat{H}(u, \nu)$ after the DCT-based denoising step (see 2.3). We can notice that two different pass-band filters, related to two different PSFs are visible on these images. We can also notice that there is no aliasing error and this first denoising step allows us to obtain the expected shape of a band-pass filter (see Eq. (5)) on which the learning step of our Gaussian mixture, exploiting the EM procedure will be achieved. The Gaussian mixture, estimated from these two spectrum data by the EM algorithm (without our additional constraint of symmetry) is shown in Figure 3. Two examples of PSF estimation with our approach are presented in Figure 4; Finally, Figure 5 shows examples of deconvolution ultrasound images using the deconvolution scheme presented at Section 3.

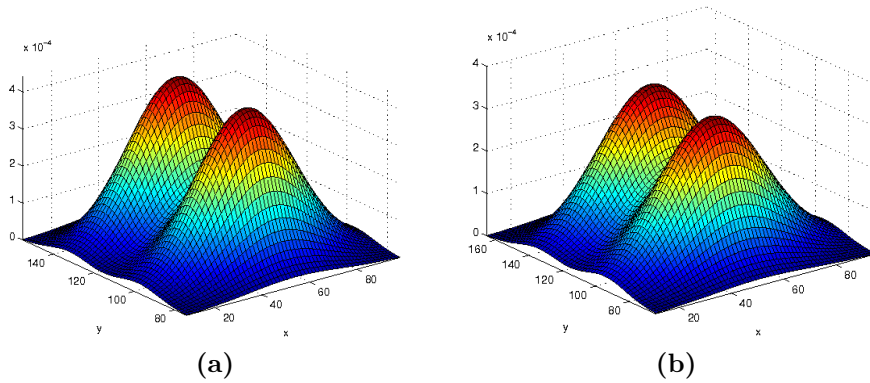


Figure 3. Surface plot of the point-spread function (PSF) defining a two-component mixture of bivariate Gaussian distributions for: (a) Fig.2a with $\mu = [54.18 \ 134.21 ; 51.82 \ 94.88]$ and $\sigma = ([358.66 \ 4.18 ; 4.18 \ 151.00], [358.84 \ 4.10 ; 4.10 \ 149.45])$, (b) Fig.2b with $\mu = [53.05 \ 131.53 ; 52.94 \ 97.40]$ and $\sigma = ([368.94 \ -5.48 ; -5.48 \ 97.40], [368.95 \ -5.47 ; -5.47 \ 96.45])$.

5. CONCLUSION

An original, simple, and fast PSF estimation strategy which is based on an additional constraint (i.e., the PSF to be estimated is of known parametric form) has been presented. With this PSF estimate, our deconvolution approach is efficiently used in order to improve the spatial resolution of the ultrasound images and to obtain an estimate of the true tissue reflectivity function which is independent of the properties of the ultrasound system. We have validated this approach with ultrasound images acquired with a portable ultrasound machine. Greater resolution improvement of the deconvolved ultrasound images was observed with substantially improved definition of the outer contour of the bone. This deconvolution method may become attractive for commercial ultrasound application due to its spatial resolution improvement or as a prerequisite stage for the segmentation and 3D reconstruction of ultrasound images.

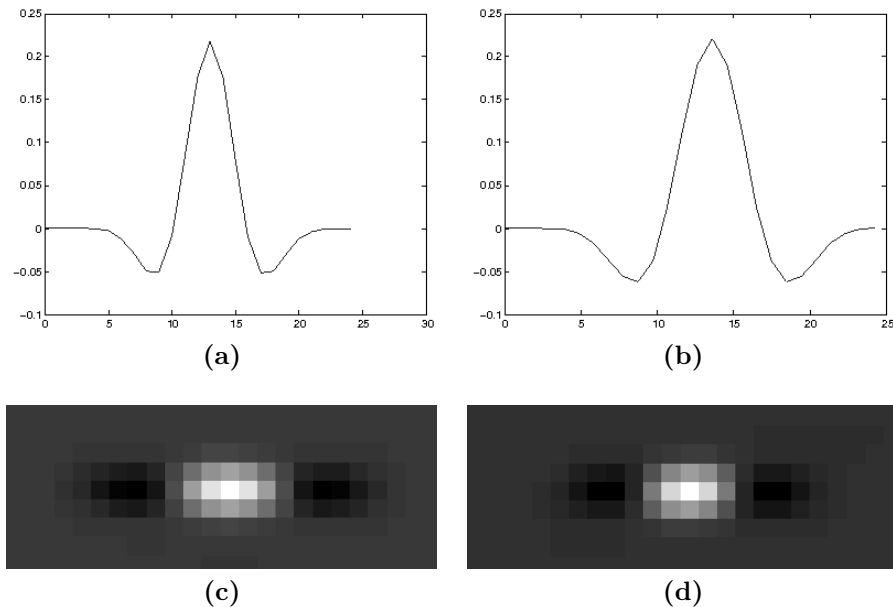


Figure 4. Estimated spectrum of the point-spread function (PSF) corresponding to respectively: (a) Fig.1a, (b) Fig.1b, (c) Fig.1a, (d) Fig.1b.

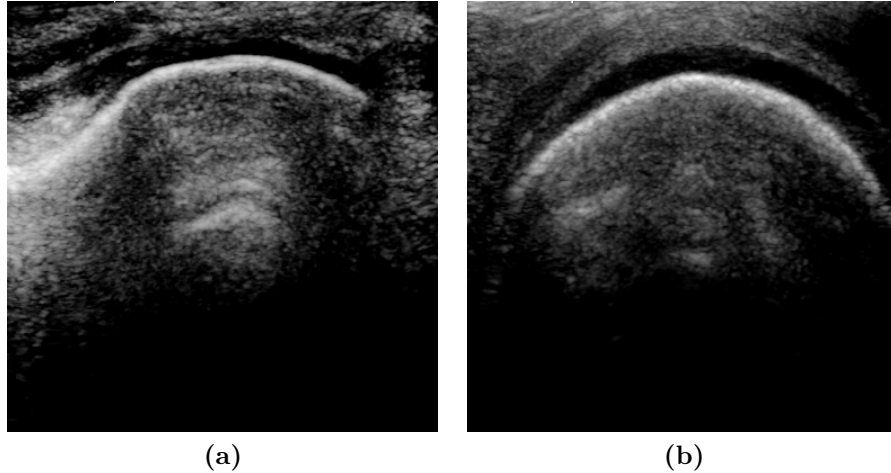


Figure 5. Deconvolved image corresponding to: (a) Fig.1a, (b) 1b.

REFERENCES

- [1] Mignotte, M., Meunier, J., Soucy, J.-P., and Janicki, C., "Comparison of deconvolution techniques using a distribution mixture parameter estimation : application in spect imagery.," *Journal of Electronic Imaging* **1**, 11–25 (January 2002).
- [2] Ayers, G. and Dainty, J., "Iterative blind deconvolution method and its application," *Optics Letters* **13**, 547–549 (July 1988).
- [3] Katsaggelos, A. and Lay, K., "Maximum likelihood blur identification and image restoration using the expectation-maximization algorithm," *IEEE Trans. on Signal Processing* **39**, 729 – 733 (March 1991).
- [4] Kundur, D. and Hatzinakos, D., "Blind image restoration via recursive filtering using deterministic constraints," in [*Proc. International Conference on Acoustics, Speech, and Signal Processing*], **4**, 547–549 (1996).
- [5] Benameur, S., Mignotte, M., Soucy, J.-P., and Meunier, J., "Image restoration using functional and anatomical information fusion with application to spect-mri images," *International Journal of Biomedical Imaging* **2009**, 12 pages (October 2009).
- [6] Cannon, M., "Blind deconvolution of spatially invariant image blurs with phase," *IEEE Transactions on Acoustics, Speech and Signal Processing* **24**, 58 – 63 (February 1976).
- [7] Abeyratne, U., Petropulu, A., and Reid, J., "Higher order spectra based deconvolution of ultrasound images," *IEEE Transactions on Ultrasonics, Ferroelectrics and Frequency Control* **42**, 1064 – 1075 (Nov. 1995).
- [8] Taxt, T., "Restoration of medical ultrasound images using two-dimensional homomorphic deconvolution," *IEEE Transactions on Ultrasonics, Ferroelectrics and Frequency Control* **42**, 543 – 554 (July 1995).
- [9] Michailovich, O. and Adam, D., "A novel approach to the 2-d blind deconvolution problem in medical ultrasound," *IEEE Trans. on Medical Imaging* **24**, 86 – 104 (Jan. 2005).
- [10] Adam, D. and Michailovich, O., "Blind deconvolution of ultrasound sequences using nonparametric local polynomial estimates of the pulse," *IEEE Transactions on Biomedical Engineering* **49**, 118 – 131 (Feb. 2002).
- [11] Dempster, A., Laird, N., and Rubin, D., "Maximum likelihood from incomplete data via the EM algorithm," *Royal Statistical Society* , 1–38 (1976).
- [12] Mignotte, M., "Fusion of regularization terms for image restoration," *Journal of Electronic Imaging* **19**, 333004– (July-September 2010).
- [13] Donoho, D. L. and Johnstone, I. M., "Ideal spatial adaptation by wavelet shrinkage," *Biometrika* **81**, 425–455 (1994).
- [14] Coifman, R. and Donohu, D., "Translation invariant denoising," in [*Wavelets and Statistics, Lecture Notes in Statistics*], **103**, 125–150, A. Antoniadis and G. Oppenheim, Eds. New York:Springer-Verlag (1995).

- [15] Kallel, F., Bertrand, M., and Meunier, J., "Speckle motion artifact under tissue rotation," *IEEE Transactions on Ultrasonics, Ferroelectrics and Frequency Control* **41**, 105 – 122 (Jan. 1994).
- [16] Mignotte, M., "A non-local regularization strategy for image deconvolution," *Journal Pattern Recognition Letters* **29**(16), 2206 – 2212 (2008).
- [17] Buades, A., Coll, B., and Morel, J. M., "A review of image denoising algorithms, with a new one," *Multiscale Modeling and Simulation (SIAM Interdisciplinary Journal)* **4**(2), 490 – 530 (2005).